Extension of Spherical Harmonic Method to RF Transient Regime

C.-K. Lin[a], Neil Goldsman[a], C.-H. Chang[a], Isaak Mayergoyz[a],
Sheldon Aronowitz[b], Jeffrey Dong[b], Nadya Belova[b]

[a]Dept. of Electrical Engineering, University of Maryland
College Park, MD 20742, USA
[b]LSI Logic Corporation, Milpitas CA, USA

Abstract

The space and time dependent electron Boltzmann transport equation (BTE) is solved self-consistently with the Poisson and transient hole current-continuity equation. A transient Spherical Harmonic expansion method is used to solve the BTE. By this method we can efficiently solve the BTE in the RF regime to observe how the complete distribution function responds to a rapid transient. Calculations on a BJT, which give the time dependent distribution function over a large energy range 0-3eV, throughout the device, as well as average quantities, require only 40 minutes CPU time on an Alpha workstation.

1. Introduction

The Spherical Harmonic method has been shown to be a viable approach for device simulation, especially when the details of the distribution function are sought[1, 2, 3, 4]. It has been used for steady state 2-D MOSFET simulation where excellent agreement with experimental values for drain current and substrate current have been obtained[5, 6]. Recently, it was shown to give excellent agreement with Monte Carlo calculations in the details of the distribution function for very deep submicron structures, while being orders of magnitude faster[6]. Until now, however, Spherical Harmonic based device simulation was limited to the steady state. In this work we extend the Spherical Harmonic method to the time-dependent situation. This extension allows one to examine how the distribution function, as well as its moments, respond to ultra-fast transient phenomena, like those which occur in very high frequency RF applications. We apply the method to provide detailed analysis of BJT transient behavior.

2. Transient Model and Numerical solution

To investigate how the distribution function responds to rapid variations of terminal voltages, we use a mathematical/physical device model which consists of the Poisson

Equation, the time-dependent Boltzmann Transport Equation for electrons, and the time-dependent Current Continuity Equation for holes.

$$\nabla_\mathbf{r}^2 \phi(\vec{r}) = \frac{q}{\epsilon_s} \left[\int f(\vec{k}, \vec{r}, t) d\vec{k} - p(\vec{r}, t) + D(\vec{r}) \right] \tag{1}$$

$$\frac{\partial f(\vec{r}, \vec{k}, t)}{\partial t} = \frac{-\nabla_\mathbf{k}}{\hbar} \varepsilon \cdot \nabla_\mathbf{r} f(\vec{k}, \vec{r}, t) - \frac{e}{\hbar} \nabla_\mathbf{r} \phi(\vec{r}) \cdot \nabla_\mathbf{k} f(\vec{k}, \vec{r}, t) + \left[\frac{\partial f(\vec{k}, \vec{r}, t)}{\partial t} \right]_c \tag{2}$$

$$\frac{\partial p(\vec{r}, t)}{\partial t} = \nabla_\mathbf{r} \cdot [\mu_p p(\vec{r}, t) \nabla_\mathbf{r} \phi(\vec{r}) + \mu_p V_t \nabla_\mathbf{r} p(\vec{r}, t)] - R(\phi, n, p) \tag{3}$$

$f(\vec{r}, \vec{k}, t)$ is the electron distribution function; $\phi(\vec{r})$ is the potential; $p(\vec{r}, t)$ is the hole concentration; $D(\vec{r})$ is the net doping concentration; $R(n, p)$ is the net hole recombination rate; $V_t = K_B T/q$ is the thermal voltage; ϵ_s is the dielectric constant of silicon. For the collision term, we explicitly evaluate the scattering integral using Fermi's Golden Rule and deformation potential theory.

In order to couple momentum space, real space and the time domain together, we first discretize these three equations in momentum and real space domains by a Scharfetter-Gummel-type discretization technique[5]. We then use a backward Euler method to discretize the time domain implicitly. The right hand side of Eqs (2,3) can be presented as $BTE(f(\vec{r}, \vec{k}, t))$, $J_p(p(\vec{r}, t))$, respectively. According to the backward Euler method, Eq(2,3) can be written as,

$$\frac{f(\vec{r}, \vec{k}, t)^{(k+1)} - f(\vec{r}, \vec{k}, t)^{(k)}}{\Delta t} = \left(BTE(f(\vec{r}, \vec{k}, t)) \right)^{(k+1)} \tag{4}$$

$$\frac{p(\vec{r}, t)^{(k+1)} - p(\vec{r}, t)^{(k)}}{\Delta t} = (J_p(p(\vec{r}, t)))^{(k+1)} \tag{5}$$

Δt is time step; $f(\vec{r}, \vec{k}, t)^{(k)}$ and $p(\vec{r}, t)^{(k)}$ are self-consistent solutions of kth step. We solve the $(k+1)'th$ time step iteratively with various approaches including of the conjugate gradient method. Due to the way we discretize the equations, $f(\vec{r}, \vec{k}, t)^{(k+1)}/\Delta t$ helps to yield a diagonally dominant system. This facilitates the use of a wide range of time-steps for stable analysis of the transient regime.

3. Results

We use the above model to perform a transient simulation of a deep submicron BJT with a base of only $0.05\mu m$. The doping profile of the BJT is shown in Fig 1(a). We first obtain a steady state solution of Eqs (1-3) for the case of $V_E = 0$, $V_B = 0$ and $V_C = 3V$. Since this is a 1D BJT case, we use a fixed V_B as a boundary condition. We then apply a step bias V_{BE}, which rises from $0V$ to $0.75V$ in 5 $psec$ to turn on the BJT and use Eqs (1,4,5) to obtain transient solution. As forward bias V_{BE} increases, the decrease in the base-emitter junction field is shown in Fig 1(b).

In Figs 2(a-c) we show the evolution of the electron energy distribution from time $t = 0$ to $t = 10 psec$, while the 0.75V bias, with rise time of $5psec$, is applied to the base. The 3D figures show the trend of the whole device. It can be seen from the 3D figures that electrons in the collector region change from being close to equilibrium to a highly heated condition in approximately $10 psec$. We also show the transient distribution function at the particular location $X = 0.2$ μm, which is the hottest point
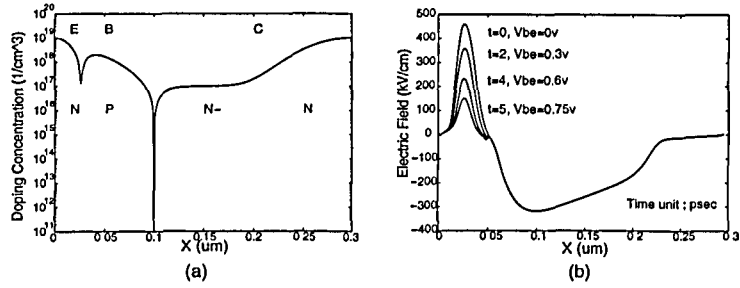
Figure 1: (a) Doping profile of BJT used in transient simulation. (b) Electric field changes for each time step.

in device, and compare the results to the quasi-static case. It is interesting to note that for $V_{BE}=0.3V$ (Fig. 2a), the BJT is still off, so right hand side device is still cool, and there are less electrons in the high-energy tail of the distribution function than would be predicted by the quasi-static calculation.

When V_{BE} first attains its maximum value (Fig. 2b), we see that the transient distribution function has overshot the quasi-static case. Finally, at $t = 10psec$, which is $5psec$ after V_{BE} reaches its maximum, the distribution has lost some of its energy to the lattice, and the transient distribution relaxes back to its quasi-static value (Fig. 2c).
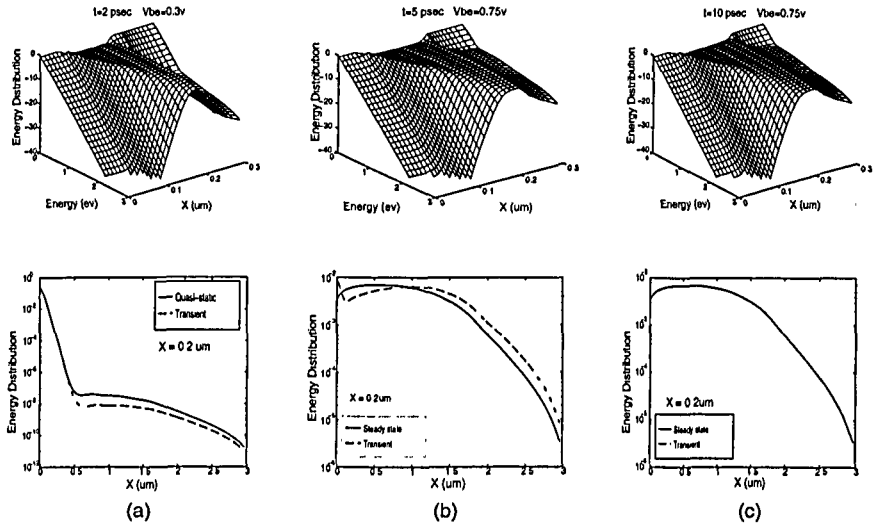
Figure 2: Evolution of the electron energy distribution and comparison with quasi-static results. (a) t=2 psec, $V_{BE}=0.3v$, BJT is still off. The number of hot electron at right hand side device is still small. (b) t=5 psec, $V_{BE}=0.75v$, BJT is on suddenly. Hot electrons emerge at right hand side device. (c) t=10 psec, $V_{BE}=0.75v$, those over-heated electrons come back to steady state.

Integrating the transient distribution function, we can observe the propagation of electrons from emitter to collector. When the voltage barrier decreases between emitter and base, electrons can not arrive at the collector instantly.

Fig. 3(a) shows the population of electrons near the collector region is less than it would be in the quasi-static case. When reaching maximum base-emitter bias, a few more time steps are required to completely transport electrons from emitter to the collector to establish a steady state. In Fig. 3(b) we show the average energy transient, which is obtained by evaluating the energy moment of the transient distribution function. It shows that during ramping up time, once we start to increase the bias, average energy in the transient case is almost always higher than it is in quasi-static case. This is because during the transient process electrons will first absorb energy from the field before they loss it to dissapative scattering processes. This results in an energy overshoot. Once we stop increasing V_{BE}, electrons get a chance to cool down and settle to their steady state value.
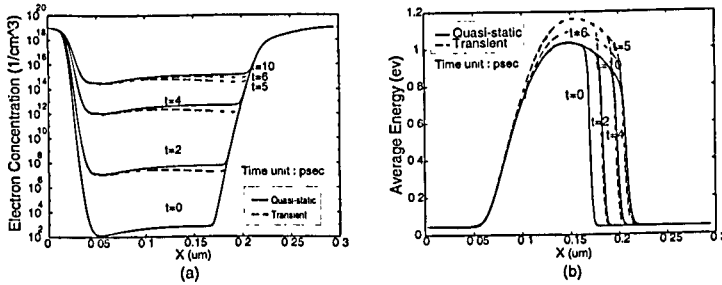
Figure 3: (a) The evolution of electron concentration and comparison with each quasi-static point. (b) The evolution of electron average energy and comparison with each quasi-static point.

References

[1] Goldsman, N.; Henrickson, L.; Frey, J, *Solid-State Electronics*, vol.34, no.4, p. 389-96,1991.

[2] A. Gnudi; D. Ventura; G. Baccarani, *Solid-State Electronics*, vol. 36, no.4, p. 575-81, 1993.

[3] K. A. Hennacy; Y.-J. Wu; N. Goldsman; I. D. Mayergoyz, *Solid-State Electronics*, vol. 38, pp. 1498–1495, 1995.

[4] Vecchi M.C.; Rudan M., *IEEE Transactions on Electron Devices*, vol.45, no.1, p. 230-8, 1998.

[5] W. Liang; N. Goldsman; I. Mayergoyz; and P. Oldiges; *IEEE Trans. on Elec. Dev.*, vol. 44, pp. 257–276, 1997.

[6] C.-H. Chang; C.-K. Lin; W. Liang; N. Goldsman; I. D. Mayergoyz; P. Oldiges; J. Melngailis, *SISPAD*, pp. 225–228, 1997.